

## APPLICATION OF NEW, HIGH-SENSITIVITY, $^1\text{H}$ - $^{13}\text{C}$ -N.M.R.-SPECTRAL TECHNIQUES TO THE STUDY OF OLIGOSACCHARIDES

LAURA LERNER AND AD BAX,

Laboratory of Chemical Physics, National Institute of Diabetes and Digestive and Kidney Diseases, National Institutes of Health, Bethesda, Maryland 20892 (U.S.A.)

(Received June 30th, 1986; accepted for publication in revised form, January 26th, 1987)

### ABSTRACT

Four n.m.r. methods that are especially useful for characterization of oligosaccharides are applied to the trisaccharide  $\alpha$ -Neu5Ac-(2 $\rightarrow$ 3)- $\beta$ -Gal-(1 $\rightarrow$ 4)-Glc (**1**). Three of these are two-dimensional, heteronuclear methods that provide chemical-shift correlation maps having much higher sensitivity than was previously possible, because they rely on indirect observation of  $^{13}\text{C}$  via  $^1\text{H}$  detection. These methods are used to assign, completely, the  $^1\text{H}$ - and  $^{13}\text{C}$ -n.m.r. spectra of both anomers of the trisaccharide. In addition to these two-dimensional methods, a one-dimensional method is used to measure  $^1\text{H}$ - $^1\text{H}$  coupling-constants accurately within each sugar ring. The values of the coupling constants thus measured for **1** are evidence that the conformations of the individual sugar rings are not affected by linkage into the trisaccharide.

### INTRODUCTION

$^1\text{H}$ -Nuclear magnetic resonance (n.m.r.) spectra of carbohydrates are notoriously difficult to analyze because of the frequent occurrence of overlapping peaks. Two-dimensional  $^{13}\text{C}$ - $^1\text{H}$  chemical shift correlation maps are usually helpful in assigning the nonanomeric proton spectra, because of the greater spread in  $^{13}\text{C}$  chemical shifts. In such a map, each peak arises from connectivity between a  $^{13}\text{C}$  nucleus (X) and a proton (H) having coordinates ( $\delta_X$ ,  $\delta_H$ ). A variety of shift-correlation experiments are available for establishing one-bond couplings<sup>1–5</sup>, long-range couplings<sup>5–7</sup>, or relayed correlation<sup>8–11</sup>. In Fig. 1, these three types of connectivity are shown schematically for a disaccharide.

As a consequence of the relative insensitivity of  $^{13}\text{C}$ , conventional heteronuclear chemical shift correlation experiments in which the observed nucleus is  $^{13}\text{C}$  require rather large amounts of pure material. If the effect of  $^{13}\text{C}$  on  $^1\text{H}$  could be observed instead of *vice versa*, a substantial gain in sensitivity would be achieved. Recently, such indirect detection methods have been developed<sup>12–14</sup>. We now demonstrate the use of three methods that rely on  $^1\text{H}$  detection, requiring  $\sim 1/10$ th to  $1/20$ th the amount of sample to obtain heteronuclear chemical shift correlation maps. Pulse sequences for all four methods used herein are shown in Fig. 2. Further

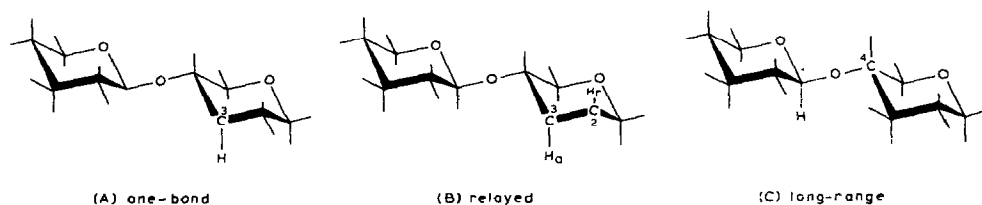


Fig. 1. Types of  $^1\text{H}$ - $^{13}\text{C}$  connectivities revealed by methods described herein. (A) One-bond correlation between a  $^{13}\text{C}$  atom at position 3 and its directly attached  $^1\text{H}$ ; (B) relayed correlation, from  $\text{H}_i$  (position 2) to  $^{13}\text{C}_i$  (position 3), via  $\text{H}_a$  (position 3); (C) long-range correlation, shown for (1 $\rightarrow$ 4)-glycosidic linkage.

experimental details (including phase cycling schemes) can be found elsewhere<sup>12-14</sup>. Summers *et al.*<sup>15</sup> have extended application of the HMQC and HMBC techniques to macromolecules, specifically a bacterial capsular polysaccharide<sup>15</sup>.

The utility of indirect detection methods will be demonstrated here by applying them to the complete assignment of the trisaccharide  $\alpha\text{-Neu5Ac-(2}\rightarrow\text{3)-}\beta\text{-Gal-(1}\rightarrow\text{4)-Glc}$  (**1**). This seemingly simple trisaccharide actually has a very complicated spectrum in which 23  $^1\text{H}$  resonances occur within 0.4 p.p.m. The complete  $^{13}\text{C}$  assignment of this compound has been published by Berman<sup>16</sup> and Sabesan and Paulson<sup>17</sup>, based on isotope shifts and comparisons with related molecules. A partial  $^1\text{H}$  assignment has been published by Haverkamp *et al.*<sup>18</sup> and Sabesan and Paulson<sup>17</sup>. We have verified the  $^{13}\text{C}$  assignment and completed the  $^1\text{H}$

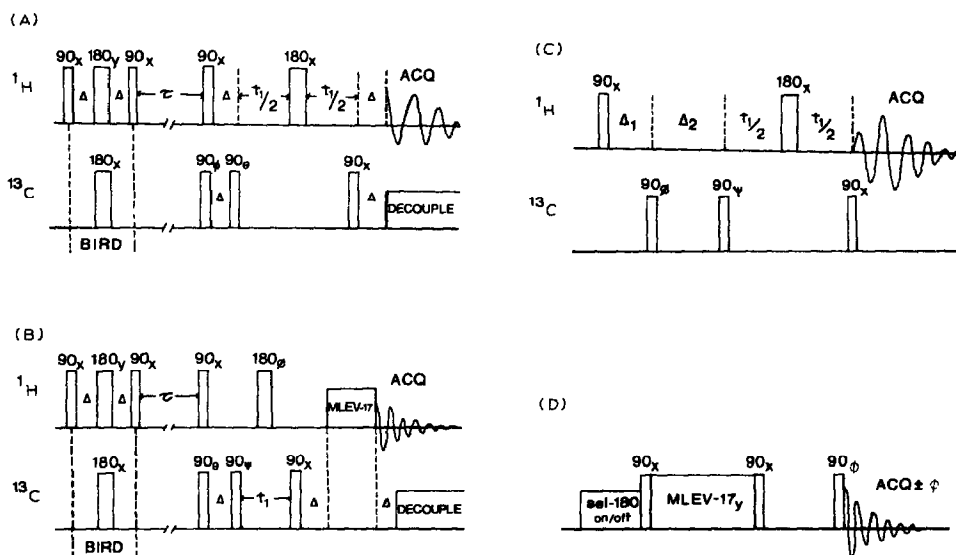


Fig. 2. Pulse sequences for the methods used in analyzing the trisaccharide **1** are (A) for obtaining one-bond,  $^{13}\text{C}$ - $^1\text{H}$  correlations (HMQC)<sup>12</sup>; (B) for obtaining relayed  $^{13}\text{C}$ - $^1\text{H}$  correlations<sup>13</sup>; (C) for obtaining long-range  $^{13}\text{C}$ - $^1\text{H}$  correlations (HMBC)<sup>14</sup>; and (D) for obtaining  $^1\text{H}$ -subspectra<sup>30</sup>.

assignments for both anomers of **1** by using  $^{13}\text{C}$ - $^1\text{H}$  correlation maps created with the three indirect detection methods to be described, using a 3.5 mg sample of **1**. Because **1** exists in aqueous solution as a 2:1 mixture of the  $\beta$  and  $\alpha$  anomers (based on integration of the anomeric protons in the one-dimensional  $^1\text{H}$  spectrum), the sample contained  $\sim 2.3$  mg of the  $\beta$  anomer and 1.2 mg of the  $\alpha$  anomer.

The three heteronuclear techniques have in common the generation and detection of multiple quantum coherence between  $^{13}\text{C}$  and  $^1\text{H}$  nuclei. The  $^1\text{H}$  signals are modulated by the  $^{13}\text{C}$  nuclei, and the final spectrum looks like a conventional ( $^{13}\text{C}$ -detected) heteronuclear correlation map. Indirect detection of a low- $\gamma$  nucleus exploits the inherently stronger signal from the ubiquitous, high- $\gamma$  proton. Instrumentation required for indirect detection consists of (1) a probe having a  $^1\text{H}$ -observe coil and a decoupler coil that can be tuned to  $^{13}\text{C}$ ; (2) a spectrometer with the capability of high-power decoupling of  $^{13}\text{C}$ ; and (3) good spectrometer stability. Stability is a requirement because alternate data acquisitions must be accurately subtracted in order to remove large residual signals from protons not coupled to  $^{13}\text{C}$  nuclei.

Once a complete proton assignment is made, scalar  $^1\text{H}$ - $^1\text{H}$  coupling constants can be measured accurately by using HOHAHA subspectral editing<sup>19</sup> with  $z$ -filtering<sup>20</sup>. The application of this method of determining coupling constants will be described after presentation of the three heteronuclear correlation techniques.

## EXPERIMENTAL

*Materials and methods.* — Compound **1** was purchased from BioCarb Chemicals, and used without purification. After lyophilization from  $^2\text{H}_2\text{O}$ , **1** (3.5 mg) was dissolved in  $^2\text{H}_2\text{O}$  (0.35 mL) (99.96%, MSD Isotopes). Spectra were obtained at  $20^\circ$  by using a probe with a tunable, broadband decoupling coil\* and a Nicolet NT500 spectrometer that had been modified to allow decoupling of  $^{13}\text{C}$  nuclei over a range of 60 p.p.m. The  $90^\circ$  pulse for  $^{13}\text{C}$  at 125.76 MHz was 100  $\mu\text{s}$ .  $^1\text{H}$ -Chemical shifts are reported relative to sodium 2,2,3,3-tetradeuterio-4,4-dimethyl-4-silapentanoate (TSP) by setting the chemical shift of residual  $^1\text{H}_2\text{O}$  to 4.820 p.p.m. at  $20^\circ$ .  $^{13}\text{C}$ -Chemical shifts are referenced to TSP by the method described in ref. 12. Additional experimental details are given in the Figure captions. The pH of the sample was 6.5, measured by electrode without correction for the difference between pH and pD.

## RESULTS AND DISCUSSION

*One-bond  $^{13}\text{C}$ - $^1\text{H}$  connectivity.* — The first experiment described here

\*Cryomagnet Systems, Inc., Indianapolis, IN.

generates a chemical shift correlation map of directly bonded  $^{13}\text{C}$ - $^1\text{H}$  pairs. Morris and Hall<sup>21</sup> first applied the conventional ( $^{13}\text{C}$ -detected), 2-D heteronuclear experiment to mono- and di-saccharides. In the conventional pulse sequence, signals from  $^{13}\text{C}$  nuclei are modulated by their one-bond scalar coupling to protons. The major obstacle in translating this method to its proton-detected equivalent is the strong, unwanted signal from protons *not* coupled to  $^{13}\text{C}$  nuclei. To circumvent this problem, the proton-detected, heteronuclear chemical shift correlation pulse-sequence (HMQC; see Fig. 2A) begins with a BIRD pulse (Bilinear Rotation<sup>12,22,23</sup>) that inverts magnetization of protons not coupled to  $^{13}\text{C}$  nuclei; magnetization of protons attached to  $^{13}\text{C}$  nuclei is not affected. After a delay  $\tau$ , calibrated to

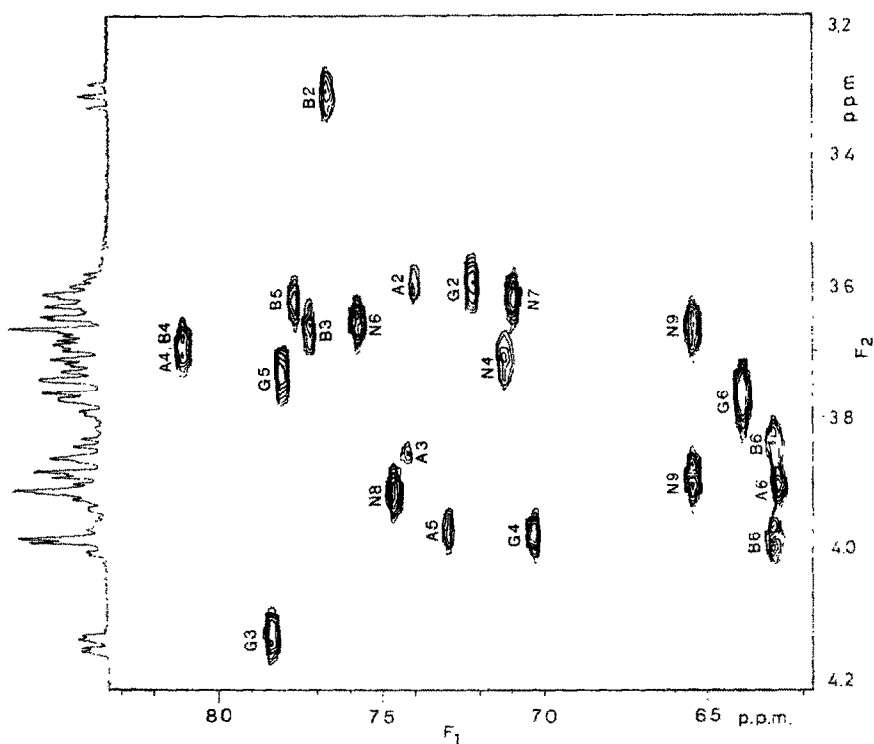


Fig. 3. Most crowded portion of the chemical shift correlation map for directly bonded  $^1\text{H}$ - $^{13}\text{C}$  pairs in **1**;  $^1\text{H}$  at 500.90 MHz and  $^{13}\text{C}$  at 125.76 MHz and  $20^\circ$ , obtained with the pulse sequence shown in Fig. 2A. The data matrix was  $2 \times 257 \times 512$  (two sets of  $257 \times 512$  data matrices collected in alternate blocks); 64 scans per  $t_1$  value (16 scans would have provided sufficient signal-to-noise). The delay between acquisitions was 0.94 s. The spectral window was  $\pm 5000$  Hz in the  $F_1$  dimension ( $^{13}\text{C}$ ), and  $\pm 1046$  Hz in the  $F_2$  dimension ( $^1\text{H}$ ); 30- and 6-Hz Gaussian linebroadenings were used in the  $t_1$  and  $t_2$  dimensions, respectively. Total measuring time was 2.4 h. The corresponding portion of the one-dimensional  $^1\text{H}$  spectrum of **1** at 500.90 MHz is displayed along the side of the two-dimensional map. Peaks are labelled with the following symbols for their assignments: N = Neu5Ac, G = Gal, A =  $\alpha$ -Glc, and B =  $\beta$ -Glc.

correspond to the zero-crossing of the inverted magnetization, the generation of multiple quantum coherence begins. Signals from protons not attached to  $^{13}\text{C}$  nuclei therefore are strongly attenuated by this saturation procedure. Any residual signal from these protons is removed by phase cycling. Spectra are recorded in the absorption mode<sup>24</sup>, so that optimal resolution and sensitivity are obtained. Fig. 3 is the most crowded region of the one-bond chemical shift correlation map for **1**, with each peak labelled with its assignment.

*Relayed connectivity.* — When a one-bond map does not suffice to assign all resonances unambiguously, a map of relayed connectivity can provide the missing links. In the conventional heteronuclear RELAY experiment, magnetization is transferred from a remotely bonded proton,  $\text{H}_r$ , to the heteronucleus, X ( $^{13}\text{C}$ ) via its coupling partner,  $\text{H}_a$ , which is directly attached to X. Each peak in a correlation map obtained in this way has the coordinates  $(\delta_{\text{H}}, \delta_{\text{X}})$ . In the analogous  $^1\text{H}$ -detected RELAY experiment described here, magnetization is transferred from X

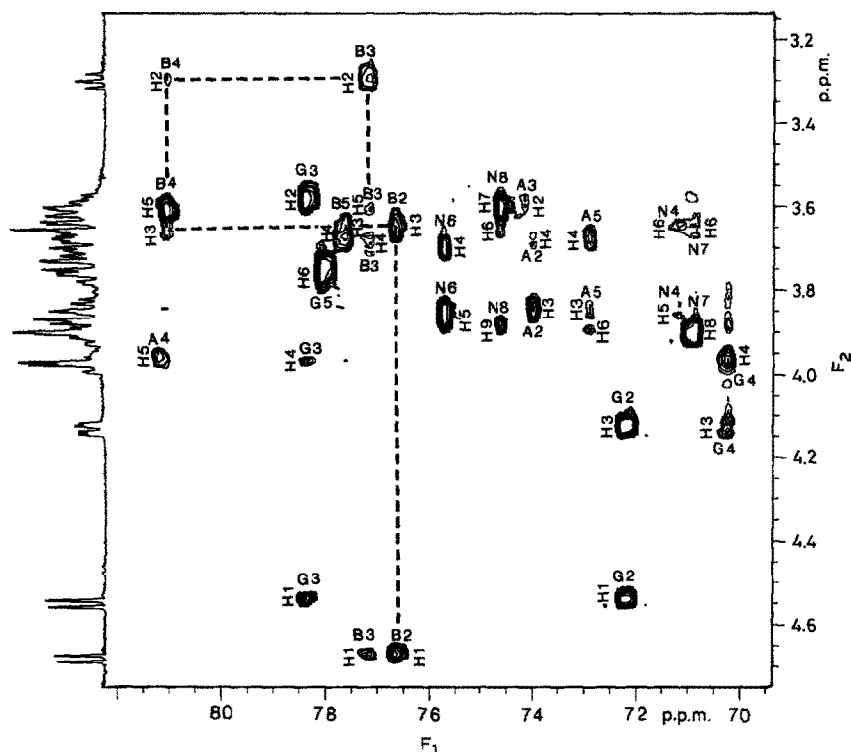


Fig. 4. Portion of chemical shift correlation map for relayed connectivities between  $^{13}\text{C}$  and  $^1\text{H}$  for **1**, obtained with the pulse sequence shown in Fig. 2B, at 500.09 MHz, and  $20^\circ$ . The data matrix was  $2 \times 297 \times 512$ , 96 scans per  $t_1$  value. The MLEV-17 mixing period was 25 ms, flanked by two 1.5-ms trim pulses. The delay time, spectral windows, and linebroadenings used were the same as in Fig. 3. Total measuring time was 10 h. Peaks are labelled with their assignments;  $\text{H}\# =$  proton attached directly to carbon number  $\#$ . The dotted line traces part of the path used to assign the  $\beta$ -Glc residue. The only incompletely suppressed direct connectivity is between Gal H-4 and Gal C-4 at 3.95, 70.37 p.p.m.

by the creation of multiple quantum coherence with  $H_a$ , and thence transferred to  $H_r$  by the homonuclear Hartmann–Hahn mechanism<sup>19,25–27</sup>. As in the one-bond experiment already described, the pulse sequence (see Fig. 2B) begins with a BIRD pulse to saturate the unwanted signals from protons not bound to  $^{13}\text{C}$  nuclei.

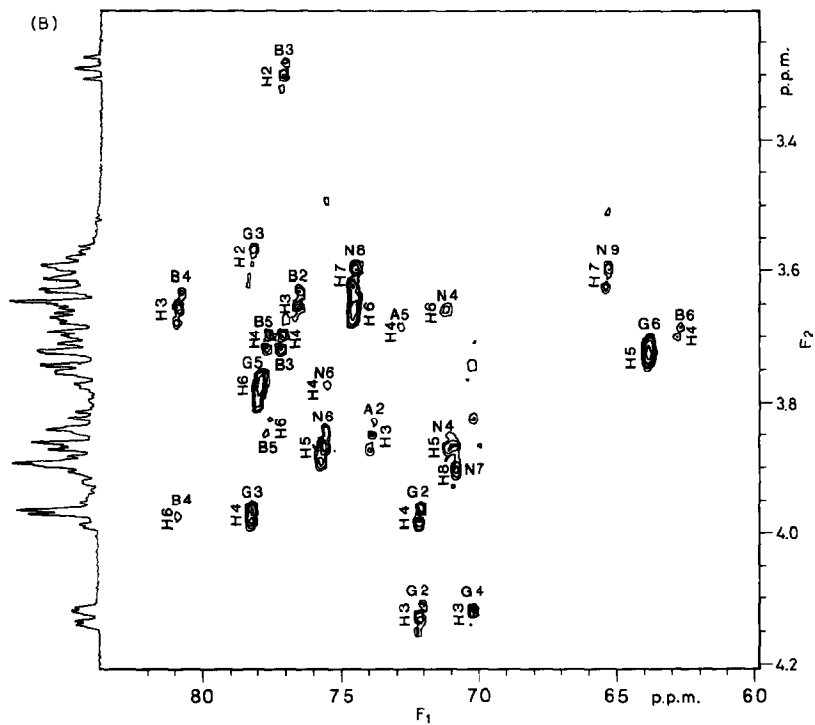
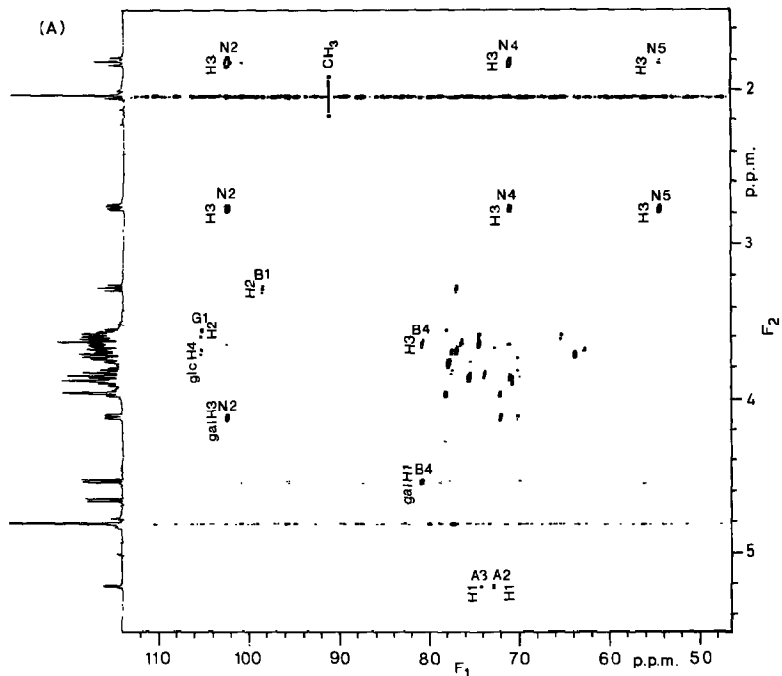
Figure 4 shows the most crowded region of the chemical shift correlation map of **1**, obtained by  $^1\text{H}$ -detected heteronuclear-relay spectroscopy. In practice, to complete the assignment of **1**, we went back and forth between the one-bond map (Fig. 3) and the relay map until the identification of direct and relayed connectivities was self-consistent. As an example, the  $^{13}\text{C}$ – $^1\text{H}$  connectivity pattern for the  $\beta$ -D-glucose residue of **1** is traced with a dotted line in Fig. 4.

*Long-range connectivity.* — The  $^1\text{H}$ -detected relay experiment can, in an overnight acquisition, yield a clear heteronuclear chemical shift correlation map for as little as 1–2 mg of a trisaccharide. One limitation on its usefulness, however, is that it does not relay magnetization across nonprotonated  $^{13}\text{C}$  nuclei or across other heteronuclei, such as oxygen. This kind of information can be obtained by determination of long-range scalar connectivity between  $^{13}\text{C}$  and  $^1\text{H}$ . Earlier versions of  $^{13}\text{C}$ -detected methods for determination of long-range heteronuclear connectivity<sup>5–7</sup> required more sample, by at least an order of magnitude, than the one-bond connectivity experiment. An additional problem with these earlier versions is that the intensity of a  $^{13}\text{C}$ – $^1\text{H}$  long-range connectivity is also a function of  $^1J_{\text{CH}}$ , which can lessen the intensity of the long-range connectivity by as much as 100%. The analogous  $^1\text{H}$ -detected experiment (HMBC) does not have this disadvantage, and it is  $\sim 20$ – $50$  times more sensitive as well. Spectrometer stability is especially critical for this long-range experiment, because the signal from protons not coupled to  $^{13}\text{C}$  nuclei cannot be presaturated by the application of a BIRD pulse and a suitable delay. Therefore, this unwanted signal must be minimized solely by phase cycling and subtraction of alternate scans (see Fig. 2C). In spite of this drawback, a long-range connectivity map is worth having in addition to a relay map because it can reveal connectivities across the glycosidic linkage, and therefore is extremely useful in sequencing oligosaccharides. It also provides a direct method for assigning nonprotonated  $^{13}\text{C}$  resonances (such as C-2 of the Neu5Ac residue of **1**), and provides an independent way in which to confirm assignments based on other techniques.

Fig. 5A is the long-range,  $^1\text{H}$ – $^{13}\text{C}$  chemical shift correlation map for **1** obtained by  $^1\text{H}$ -detection; Fig. 5B is the most crowded region of that map,

---

Fig. 5. (A) Complete chemical shift correlation map of long-range connectivities between  $^1\text{H}$ – $^{13}\text{C}$  pairs in **1**, at 500.09 MHz and  $20^\circ$ . The map was generated with the pulse sequence shown in Fig. 2C. The spectral window was  $\pm 5000$  Hz in the  $F_1$  dimension ( $^{13}\text{C}$ ), and  $\pm 1200$  Hz in the  $F_2$  dimension ( $^1\text{H}$ ). The absolute value mode spectrum originated from a  $297 \times 1024$  data matrix with 128 scans per  $t_1$  value. Total measuring time was 16 h. Peaks arising from long-range couplings across the glycosidic bonds are labelled as follows: (gal H3, N2), (glc H4, G1), (gal H1, B4). Incompletely suppressed  $^1J_{\text{CH}}$  correlation between the methyl protons and the methyl  $^{13}\text{C}$  resonance (folded in the  $F_1$  dimension) is indicated by a vertical bar. (B) The most crowded region of (A), with every peak labelled with its assignment.



expanded to show the assignments. The interglycosidic connectivities between Neu5Ac C-2 and Gal H-3, and between Gal C-1 and Glc H-4, and  $\beta$ Glc C-4 and Gal H-1, are seen clearly in Fig. 5A. This method is sensitive enough to reveal the long-range coupling between  $\alpha$ Glc C-1 and  $\alpha$ Glc H-2, H-3 in an overnight acquisition, even though the sample contained only  $\sim 1.2$  mg of the  $\alpha$  anomer.

The complete  $^1\text{H}$ - $^{13}\text{C}$  assignments of **1** (with the exception of C-1,  $\text{CH}_3\text{CO}$ , and  $\text{CH}_3\text{CO}$  of Neu5Ac, whose chemical shifts are outside the range covered by the  $^{13}\text{C}$  decoupling used in these experiments) are listed in Tables I and II. These

TABLE I

 $^1\text{H}$ -CHEMICAL SHIFTS (P.P.M.) FOR **1** AT 500.09 MHz AND 20°, FROM TSP

Position	Residue			
	Neu5Ac	Gal	$\beta$ -Glc	$\alpha$ -Glc
1		4.56	4.66	5.21
2		3.57( $\alpha$ ) <sup>a</sup> 3.56( $\beta$ )	3.28	3.57
3	1.80( <i>a</i> ) 2.75( <i>e</i> )	4.11( $\alpha$ ) 4.10( $\beta$ )	3.63	3.83
4	3.68	3.95	3.67	3.66
5	3.85	3.75	3.59	3.95
6	3.65	3.77	3.83 3.96	3.90
7	3.62			
8	3.93			
9	3.68 3.89			
CH <sub>3</sub>	2.03			

<sup>a</sup>Gal H-2 and H-3 exhibit two chemical shifts, dependent upon the anomeric form of the attached Glc residue.

TABLE II

 $^{13}\text{C}$ -CHEMICAL SHIFTS (P.P.M.) FOR **1** AT 125.76 MHz AND 20°, FROM TSP

Position	Residue			
	Neu5Ac	Gal	$\beta$ -Glc	$\alpha$ -Glc
1		105.32	98.63	94.61
2	102.30	72.30	76.73	74.14
3	42.73	78.45	77.25	74.30
4	71.10	70.37	81.05	81.06
5	54.68	78.09	77.71	73.01
6	75.81	64.17	62.99	62.98
7	70.99			
8	74.72			
9	65.56			

assignments are in agreement with the previously published ones<sup>16,17</sup>, except for Gal C-3 and C-5, as noted later. Slight differences probably arise from differences in pH and temperature, in addition to the difference in the chemical shift standards used. Recently, Sabesan and Paulson<sup>17</sup> reversed the tentative assignments that Berman<sup>16</sup> had proposed for Gal C-3 and C-5, and our assignments confirm this reversal. We observed that Gal H-6a and H-6b have the same chemical shift (3.77 p.p.m.), as do  $\alpha$ Glc H-6a and H-6b (3.90 p.p.m.)

$^1\text{H}$ - $^1\text{H}$  Coupling constants. — Karplus relations between the value of vicinal coupling constants and bond angles are a valuable source of information about conformation<sup>28,29</sup>. The difficulty in measuring coupling constants for nonanomeric protons has limited their use in conformational analysis of carbohydrates. Once proton chemical shift assignments are in hand, it is possible to measure accurately the scalar coupling-constants for many  $^1\text{H}$ - $^1\text{H}$  pairs within each sugar ring of an oligosaccharide by using the method suggested by Subramanian and Bax<sup>30</sup>. The method consists of generating a subspectrum of each spin system, and removing dispersive components of the magnetization that otherwise would distort the final lineshape. One resonance, usually the anomeric proton since it is well separated from the others, is selectively inverted, and its magnetization is transferred within its coupled spin-system by the homonuclear Hartmann-Hahn mechanism (see Fig. 2D). Signals from multiple-quantum transitions are removed by phase cycling; and signals from zero-quantum transitions are removed by applying a z-filter<sup>20</sup>. The resulting subspectrum can be phased to pure absorption, allowing direct measurement of scalar coupling constants. Tracing of the coupling network proceeds until halted by a small ( $< \sim 1$  Hz) coupling constant between protons, through which transfer of magnetization does not progress at a significant rate.  $^1\text{H}$ - $^1\text{H}$  Coupling constants determined in this way for **1** are listed in Table III. For

TABLE III

 $^1\text{H}$ - $^1\text{H}$  COUPLING CONSTANTS<sup>a</sup> (Hz) FOR **1**

$^1\text{H}$ - $^1\text{H}$ Pair	Residue			
	Neu5Ac	Gal	$\beta$ -Glc	$\alpha$ -Glc
$J(1,2)$		7.84(7.89)	7.95(7.95)	3.75(3.75)
$J(2,3)$		9.0(9.92)	9.19(9.22)	9.90(9.90)
$J(3,3)$	-12.49(-13.07)			
$J(3,4)$	a 11.49(12.30) e 4.54(4.95)	3.14(3.48)	10.00(9.06)	9.49(9.6)
$J(4,5)$	10.39(10.2)	1.5(1.5)	10.00(9.8)	10.00(9.6)
$J(5,6)$	9.91(10.3)		1.79(2.05)	1.5(2.2)
$J(6,7)$	1.68(1.5)			

<sup>a</sup>Values in parentheses are  $^1\text{H}$ - $^1\text{H}$  coupling constants for the corresponding monosaccharides, obtained by inspection of one-dimensional spectra recorded at 500.09 MHz and 20°. In solution, sialic acid (Neu5Ac) occurs as a 93:7 mixture of  $\beta$ : $\alpha$  anomers<sup>33</sup>, and so the coupling constants in parentheses are for the  $\beta$  anomer.

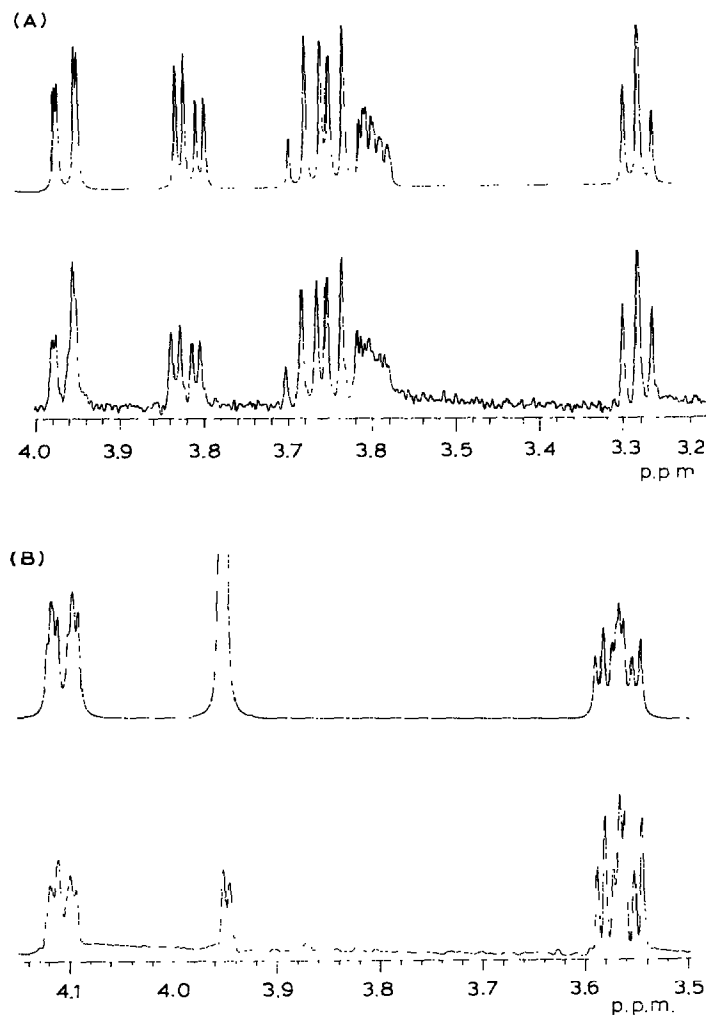


Fig. 6. Subspectra obtained with the z-filtered HOHAHA pulse-sequence shown in Fig. 2D, with an MLEV-17 mixing time of 210 ms. (A)  $\beta$ -Glc residue, H-1 resonance at 4.65 p.p.m. inverted; top, simulated subspectrum; bottom, experimental spectrum. (B) Gal residue, H-3 resonance at 4.105 p.p.m. inverted; top, simulated subspectrum; bottom, experimental spectrum. Simulation was based on the existence of two sets of Gal H-2 and H-3 atoms, corresponding to 2:1  $\beta$ : $\alpha$  anomers of Glc. Spectra were simulated with the NMRSIM program provided by GE-Nicolet in its 1280 software package.

comparison,  $^1\text{H}$ - $^1\text{H}$  coupling constants for the monosaccharides  $\beta$ -sialic acid ( $\beta$ -Neu5Ac, the preponderant species in solution),  $\beta$ -D-galactose, and  $\alpha$ - and  $\beta$ -D-glucose are also listed in Table III.

Two examples of experimental and simulated subspectra (based on the coupling constants and chemical shifts listed in Tables I and III) are shown in Fig. 6. Values of the coupling constants for **1** are within 1 Hz of values for both the free monosaccharides that we measured at 500 MHz and for the  $\beta$  anomer of **1** bound

to a ceramide (ganglioside  $\text{G}_{\text{M3}}$ ; see ref. 31). This is evidence that the conformations of the individual sugar rings are not affected when linked in a trisaccharide; or, in turn when the trisaccharide is bound to a ceramide.  $^1\text{H}$ - $^1\text{H}$  Coupling constants can also be obtained by  $J$ -resolved spectroscopy<sup>32</sup>, but in practice it is difficult to analyze the spectra obtained with this method in the presence of strong coupling or multiple overlapping resonances. Measuring coupling constants by generating simpler subspectra should increase the feasibility of studying oligosaccharide conformations by  $^1\text{H}$ -n.m.r. spectroscopy. The subspectrum of the Gal residue (see Fig. 6B) is best simulated by assuming that protons 2 and 3 exhibit significantly different chemical shifts, depending upon which anomeric form of Glc is attached. In the  $\beta$  anomer, H-2 and H-3 are shifted slightly (0.007 p.p.m.) upfield. Gal H-4 may also have two slightly different shifts, because its linewidth is slightly larger than that of the other resonances. Gal  $J_{1,2}$  and  $J_{2,3}$  are not significantly different for the two anomers. This subtle change in chemical shift would be nearly impossible to detect in an oligosaccharide without generating a subspectrum of the Gal residue.

The pulse sequences described herein make it possible to analyze completely the  $^1\text{H}$ - and  $^{13}\text{C}$ -n.m.r. spectra of as little as 1–2 mg of an oligosaccharide in a reasonable length of time. Generation of a one-bond,  $^1\text{H}$ - $^{13}\text{C}$  chemical-shift correlation map and HOHAHA subspectra is possible for much smaller quantities. These methods should prove very useful in the analysis of oligosaccharides, especially when only a limited amount of a pure sample is available.

#### ACKNOWLEDGMENTS

We thank Rolf Tschudin for his excellent technical assistance. L. Lerner was supported by an Arthritis Foundation Postdoctoral Fellowship.

#### REFERENCES

- 1 A. A. MAUDSLEY, L. MÜLLER, AND R. R. ERNST, *J. Magn. Reson.*, 28 (1977) 463–469.
- 2 G. BODENHAUSEN AND R. FREEMAN, *J. Magn. Reson.*, 28 (1977) 471–476.
- 3 A. A. MAUDSLEY AND R. R. ERNST, *Chem. Phys. Lett.*, 50 (1977) 368–372.
- 4 A. BAX AND S. K. SARKAR, *J. Magn. Reson.*, 60 (1984) 170–176.
- 5 A. BAX, in G. C. LEVY (Ed.), *Topics in Carbon-13 NMR*, Wiley, New York, 1984, ch. 8.
- 6 H. KESSLER, C. GRIESINGER, J. ZARBOCK, AND H. R. LOOSLI, *J. Magn. Reson.*, 57 (1984) 331–336.
- 7 H. KESSLER, W. BERMEL, AND C. GRIESINGER, *J. Am. Chem. Soc.*, 107 (1985) 1083–1084.
- 8 P. H. BOLTON, *J. Magn. Reson.*, 48 (1982) 336–340.
- 9 P. H. BOLTON, *J. Magn. Reson.*, 54 (1983) 333–337.
- 10 A. BAX, *J. Magn. Reson.*, 53 (1983) 149–153.
- 11 H. KESSLER, M. BERND, H. KOGLER, J. ZARBOCK, O. W. SØRENSEN, G. BODENHAUSEN, AND R. R. ERNST, *J. Am. Chem. Soc.*, 105 (1983) 6944–6952.
- 12 A. BAX AND S. SUBRAMANIAN, *J. Magn. Reson.*, 67 (1986) 565–569.
- 13 L. LERNER AND A. BAX, *J. Magn. Reson.*, 69 (1986) 375–380.
- 14 A. BAX AND M. F. SUMMERS, *J. Am. Chem. Soc.*, 108 (1986) 2093–2096.
- 15 R. A. BYRD, W. EGAN, M. F. SUMMERS, AND A. BAX, *Carbohydr. Res.*, 166 (1987) 47–58.
- 16 E. BERMAN, *Biochemistry*, 23 (1984) 3754–3759.
- 17 S. SABESAN AND J. C. PAULSON, *J. Am. Chem. Soc.*, 108 (1986) 2068–2080.

- 18 J. HAVERKAMP, H. VAN HALBEEK, L. DORLAND, J. F. G. Vliegenthart, R. Pfeil, and R. Schauer, *Eur. J. Biochem.*, 122 (1982) 305-311.
- 19 D. G. DAVIS AND A. BAX, *J. Am. Chem. Soc.*, 107 (1985) 7197-7198.
- 20 O. W. SØRENSEN, M. RANCE, AND R. R. ERNST, *J. Magn. Reson.*, 56 (1984) 527-534.
- 21 G. A. MORRIS AND L. D. HALL, *J. Am. Chem. Soc.*, 103 (1981) 4703-4711.
- 22 J. R. GARBOW, D. P. WEITEKAMP, AND A. PINES, *Chem. Phys. Lett.*, 93 (1982) 504-509.
- 23 A. BAX, *J. Magn. Reson.*, 52 (1983) 330-334.
- 24 J. STATES, R. S. HABERKORN, AND D. J. RUBEN, *J. Magn. Reson.*, 48 (1982) 286-292.
- 25 L. BRAUNSCHEWILER AND R. R. ERNST, *J. Magn. Reson.*, 53 (1983) 521-529.
- 26 A. BAX AND D. G. DAVIS, *J. Magn. Reson.*, 63 (1985) 207-213.
- 27 D. G. DAVIS AND A. BAX, *J. Am. Chem. Soc.*, 107 (1985) 2820-2821.
- 28 C. A. G. HAASNOOT, F. A. A. M. DELEEUW, AND C. ALTONA, *Tetrahedron*, 36 (1980) 2783-2792.
- 29 C. ALTONA AND C. A. G. HAASNOOT, *Org. Magn. Reson.*, 13 (1980) 417-429.
- 30 S. SUBRAMANIAN AND A. BAX, *J. Magn. Reson.*, in press.
- 31 T. A. W. KOERNER, JR., J. H. PRESTEGARD, P. C. DEMOU, AND R. K. YU, *Biochemistry*, 22 (1983) 2676-2687.
- 32 W. P. AUE, J. KARHAN, AND R. R. ERNST, *J. Chem. Phys.*, 63 (1976) 4226-4227.
- 33 E. B. BROWN, W. S. BREY, JR., AND W. WELTNER, JR., *Biochim. Biophys. Acta*, 399 (1975) 124-130.